ACOUSTIC SPECTROSCOPY OF MATERIALS AND STRUCTURES FOR ELECTRICAL ENGINEERING

Peter BURY

Department of Physics, Faculty of Electrical Engineering, University of Žilina,
Univerzitná 1, 010 26 Žilina, Slovak Republic

ABSTRACT

The methods of acoustic spectroscopy are powerful tool for the study physical properties of condensed matter. The ability of these methods makes it possible to obtain important information for variety of materials concerning not only their mechanical properties. The theoretical principles of acoustic spectroscopy of some kinds of materials and structures perspective for application in electrical engineering as results of a interaction of acoustic wave and charge curriers are presented. Solid glassy electrolytes, semiconductor structures and magnetic fluids are the representative selection of materials manifested the convenience of acoustic spectroscopy methods to obtain some important physical parameters.

Keywords: acoustic spectroscopy, semiconductor structures, solid electrolytes, magnetic fluids

1. INTRODUCTION

The important role played by physical acoustics in the continuing development of our understanding of the physics of solids is evident. Atoms that have combined to form a crystalline or amorphous solid constitute a medium capable of propagating all kinds of mechanical vibrations, some of them can also propagate through liquids. The low-frequency branches of the vibrational spectra can be treated as acoustic waves propagating in a continuous medium, since they have wavelengths that are much larger than the sizes and spacing of the atoms. In addition to frequency, the characteristic parameters of these waves include phase velocity, attenuation, wavelength, amplitude and polarization. By measuring these parameters as a function of temperature, frequency, electric or magnetic field, illumination representing the methods of acoustic spectroscopy a great variety of information about the physical properties of the material under investigation can be obtained.

One might think that only the mechanical properties of solids can be studied in these kinds of experiments. In fact, much more can be learned through the proper application of the methods of physical acoustics [1,2].

And, of course, it goes almost without saying that acoustic techniques have one more great advantage: acoustic waves propagate in metals as well as in dielectrics or semiconductors, contrary to the situation for electromagnetic waves. Thus acoustic methods make it possible to obtain much more information for a wide variety of solids than how they respond to quasistatic mechanical forces.

In this contribution we present mainly the principle of acoustic spectroscopy of some kinds of materials and structures perspective for application in electrical engineering as a result of the interaction between acoustic wave and charge curriers (both electrons and ions) in solids (ion conductive glasses and semiconductor structures) or magnetic particles in magnetic fluids. The results obtained on investigated materials are presented and discussed, too.

2. THEORETICAL DESCRIPTION OF ACOUSTIC SPECTROSCOPY PRINCIPLES

2.1. Relaxation properties of ion conductive glasses

Ion conductive materials designated also as solid electrolytes come to the forefront of scientific interest because of application in electrochemical devices, such as solid-state batteries, electrochronic displays and sensors. Solid electrolytes present numerous potential advantages over liquid electrolytes and the possibility for miniaturization. Fast ionic conductivity can be observed also in many glasses, especially those with small cations, such as silver, copper, lithium, and sodium. Ternary glasses contain a network former (e.g., SiO_2, B_2O_3, P_2O_5, and GeS_2), a network modifier (e.g., Ag_2O, Li_2O, Cu_2O, and Ag_2S), and a dopant compound, mostly a halide (e.g., AgI, CuI, and $LiCl$) [3,4].

Characterization of dynamic processes in glassy materials with ionic conductivity is very important since the ion transport significantly affects their practical utilization. Acoustic spectroscopy is one of the powerful techniques for the study of sub-T_g relaxations in glasses due to a strong acousto-ionic interaction [5,6]. Relaxation processes occurring on different time scales can be detected in one experiment since the corresponding acoustic loss peaks are spread out on the temperature scale.

The investigation of acoustic spectra of ionic glasses can reflect the basic features of the relaxation and transport mechanisms of the mobile ions. Acoustic measurements made over a wide range of frequencies and temperatures can characterize different relaxation processes according to corresponding transport mechanisms due to the mobile ions considering also different kinds of sites.

In the case of systems containing a low concentration of mobile ions the attenuation may be described as a superposition of Debye-like single relaxation time processes in which the individual ion hops occur independently of each other. The acoustic attenuation will exhibit a maximum when the relaxation time τ is

comparable to the period ($1/\omega$) of the acoustic perturbation, where

$$\tau = \tau_0 \exp\left(E_a / k_B T_{peak}\right) \qquad (1)$$

is the most probable relaxation time [6]. The relaxation processes, described by an Arrhenius equation (1), are characterized by activation energy E_a for jumps over the barrier between two potential minima and typical relaxation frequency of ion hopping $1/\tau_0 \approx 10^{13} - 10^{14}$ s^{-1}.

In fact all the investigated relaxation peaks are much broader than Debye peak. It can be interpreted as arising from the existence of a distribution of relaxation times due to random deviations in the local arrangement of the system. As a consequence, the τ distribution can be connected with a distribution of activation energies E_a, representing the heights of the barriers that the ions must surmount to go into the near allowed positions.

The relaxation phenomena observed in a wide variety of materials exhibit a power-law type of frequency dependence. The relationship to Debye behaviour is expressed for the acoustic attenuation α in the form [5]

$$\alpha \approx \frac{1}{T}\left(\frac{(\omega\tau)^m}{1+(\omega\tau)^{1+m+n}}\right), \qquad (2)$$

where m and n are power-law exponents, which take values between 0 and 1. When $m = 1$ and $n = 0$, equation (2) reduces to the equation for a single Debye-like process.

Two functions have mainly been used to fit mechanical loss data. The first function is the Kohlrausch-Williams-Watts (KWW) function

$$\Phi(t,T) = \exp\left[-\left(\frac{t}{\tau}\right)^{\beta}\right] \qquad (3)$$

with $0 < \beta \le 1$. The acoustical attenuation is then given by

$$\alpha(\omega,T) \propto \int_0^{\infty} \left(-\frac{d\Phi(t)}{dt}\right)\sin(\omega t)\ dt . \qquad (4)$$

The second function is the double power law

$$\alpha(\omega,T) \propto \frac{1}{(\omega\tau)^{-n}+(\omega\tau)^m} , \qquad (5)$$

which responses, as it has been demonstrated [5], can be produced by a simple exponential distribution of relaxation times.

2.2. Acoustoelectric effect on semiconductor interfaces

The semiconductor interfaces in a metal-semiconductor contacts, semiconductor-insulator interfaces and semiconductor heterostructures are the important concepts in semiconductor devices and circuits that play a revolutionary role in microeletrronics. Several useful methods have been developed during last years to study interface properties.

Recently, the acoustoelectric (AE) effect in semiconductor structures has been shown to be an effective tool also for the characterization of electrical properties and experimental study of semiconductor surfaces and interfaces. The AE interactions were applied to surface and interface state determination, carrier transport properties characterization including conductivity and carrier mobility measurement, 2D and 1D electron or hole system investigation and number of important devices utilization.

When the AE effect in semiconductor structures has been shown to be a useful tool for the experimental study of deep centers, two basic modifications of acoustoelectric (acoustic) deep-level transient spectroscopy (A-DLTS) were introduced. The former surface acoustic wave (SAW) technique uses a nonlinear AE interaction between the SAW electric field and the free carriers in an interface region which generates a transverse AE signal (TAS) across the structure. Transient measurements of the rise or fall times of the resulting dc part of the TAS [7] and later hf part of TAS have been used to study interface traps [8]. The latter longitudinal acoustic wave (LAW) technique uses an acoustoelectric response signal (ARS) observed at the interface of the semiconductor structure when a longitudinal acoustic wave propagates through the structure [9,10].

The non-destructive A-DLTS technique using SAW is based on the fact that the electric field accompanied the SAW on a piezoelectric substrate can produce due to the interaction with the free curriers the TAS that reflects any changes in the space charge distribution in the interface regions. Transverse force due to the AE interaction influences carriers in the interface region, so that the dc transverse AE voltage (TAV) is produced by space charge in the semiconductor or semiconductor structure. The resulting TAS across the structure includes dc AE effect and hf wave propagation properties and can be expressed by the relation

$$E = E_0 + E_1 e^{-i(\omega t - kx)} , \qquad (6)$$

where E_0 is dc part and E_1 is the amplitude of hf part of TAS, respectively. The corresponding carrier concentration follows the relation

$$n = n^0 + n_0 + n_1 e^{i(\omega t - kx)} , \qquad (7)$$

where n^0 is the carrier concentration with no applied field and n_0, n_1 are the AE term and term proportional to the amplitude of exciting wave, respectively.

Transversal hf ARS signal can be then given by the relation

$$U_{ac} = \int_0^{d} E_{1y} \sin(\omega t - kx)\, dx . \qquad (8)$$

Here d is the selected window width. Choosing the interaction space of the $\lambda/2$ length [or $(2n+1)\ \lambda/2$] in x direction, where n is the natural number, the average value is not zero anymore and reaches its maximum.

The basic principle of an ARS signal creation can be explained using the idea of an acoustic wave passing through the semiconductor with the space charge region characterized by a non-zero electric field, typical for example for p-n junctions, Schottky diods, MIS structures and heterostructures. The acoustic wave, following the pressure modulation of charge density evokes the change of the potential difference that manifests as an ARS signal. The ARS produced by a semiconductor structure propagating by LAW can be then expressed using the similarity with the case of electromechanical capacitance transducer of thin planar structure ($d<<\lambda$) [9] by the relation

$$U_{ac} = \frac{Q}{C_i}\frac{p}{K_i} + \frac{Q}{C_\omega}\frac{p}{K_\omega} \qquad (9)$$

where in the case of MIS structure C_i, C_ω are the capacitances of insulator and space charge region, Q is the accumulated charge, p is the acoustic pressure and K_i and K_ω are the elastic moduli of the structure layers.

The principle of A-DLTS techniques is based then on the fact that the amplitude of the measured AE signal (both TAS and ARS) is proportion to the nonequilibrium carrier density, $U_{ac} \approx \Delta n(t)$. After an injection pulse has been applied to the semiconductor the decay time constant associated with the relaxation of the AE signal amplitude is a direct measure of the time constant associated with the relaxation processes of injected carriers. The release of carriers from deep center levels that leads to the thermal equilibrium on a new steady state and has the time dependence [10]

$$U_{ac}^{0}(t) = U_0 \exp\left(-t/\tau\right) \qquad (10)$$

where U_o represents the ARS due to the AE field and τ is the time constant associated with the release of the carrier from deep centers when injection pulse is turned off. Since this relation was obtained assuming only one deep center, the result can be readily generalized.

2.3. Acoustic spectroscopy of magnetic fluids

A magnetic fluid is a colloidal suspension of magnetic particles covered with a surfactant layer in a carrier liquid. Due to the magnetic dipol-dipol interaction between the particles, the chains and chain-like elongated clusters are formed, which results in magneto-mechanical and magneto-optical effects, magneto-dielectric behavior etc. The magnetic fluids based on transformer oil have new opportunities of application in HV transformers.

Among convenient and effective methods of investigation of magnetic fluids belongs the acoustic spectroscopy. This study is undertaken to check the effect of the time of the magnetic fluid exposure to an external magnetic field to determination of dispersions characteristics, their magnitude and concentration. The stability and the structure of magnetic fluid are very important parameters of their next application as in medicine or electrical technologies [11].

When an acoustic hf wave propagates through a colloidal dispersion, it can be absorbed via a number of

mechanisms, depending on the contrast in thermophysical properties between the dispersed and continuous phases. When the acoustic wave length λ is much longer than the particles radius r ($\lambda>>r$) the acoustic attenuation α of the suspension of particles in the carrier liquid depends on the intrinsic absorption, viscoinertial absorption, thermal absorption and the scattering losses[12]. The magnetic fluid viscosity is one of the main factors determining the acoustic wave attenuation

$$\alpha_{\exp} = \frac{2\pi^2 f^2}{\rho c^3}\left(\frac{4}{3}\eta_S + \eta_V\right) \qquad (11)$$

where ρ is the density, c is the ultrasonic wave velocity, f is the frequency of the acoustic wave, η_S is the shear viscosity and η_V is the volume viscosity. The term related to thermal conductivity can be neglected for the majority of ferrofluids. When a ferrofluid is subjected to a constant magnetic field its viscosity increases (due to magnetoviscous effects) and becomes anisotropic because of the magnetic moment **m** of the particles will try to align with the magnetic field direction **H** and the particles tend to aggregate (make chain-like clusters). In the magnetic fluid studied mostly no large aggregates were detected so the increase in viscosity is explained only by ordering of the magnetic moments of the particles.

However, with increasing intensity of the field, in some fluids is a significant increase in the acoustic attenuation α, which is a result of aggregation of magnetic particles. The aggregation of particles into chain-like clusters, induced by an external magnetic field, leads to an increase in the ferrofluid viscosity and thus also in the acoustic absorption. The additional maxima of $\Delta\alpha$ appear as a result of the additional resonance absorption of the acoustic wave by the spherical clusters (the energy of the wave is transferred to the translational and rotational degree of freedom of the clusters) [11].

3. EXPERIMENTAL DETAILS

3.1. Phosphate glasses investigation

Phosphate glasses containing Cu^+ conducting ions have gained attention during few last decades because of their promising potential use in various technological applications. Conductivities comparable to Ag^+ ion-containing glasses were obtained just in corresponding systems with Cu^+ conductive ions. These glasses have been mainly prepared in systems based on P_2O_5 and/or MoO_3 [4,13]) as "glass-forming" oxides.

The acoustic relaxation processes were investigated on ionic phosphate glasses prepared in two systems, (18.18–x) CuI – x CuBr – 54.55 Cu_2O – 27.27 P_2O_5 with the step $\Delta x = 2.275$ (System I) and (25.00–y) CuI – y CuBr – 46.875 Cu_2O – 9.375 P_2O_5 – 18.750 MoO_3 with the step $\Delta y = 3.125$ (System II). Both systems were completely investigated and the procedure of their preparation have been already described [4,14,15].

The acoustic attenuation of ion conductive glasses was measured using MATEC Modulator and Receiver together with Attenuation Recorder. The longitudinal acoustic waves of frequency 13, 18 and 27 MHz were generated by

quartz transducer and measurement were made in the temperature range of 140-380 K. The quartz buffer was used to separate the signal from quite short sample (Fig. 1).
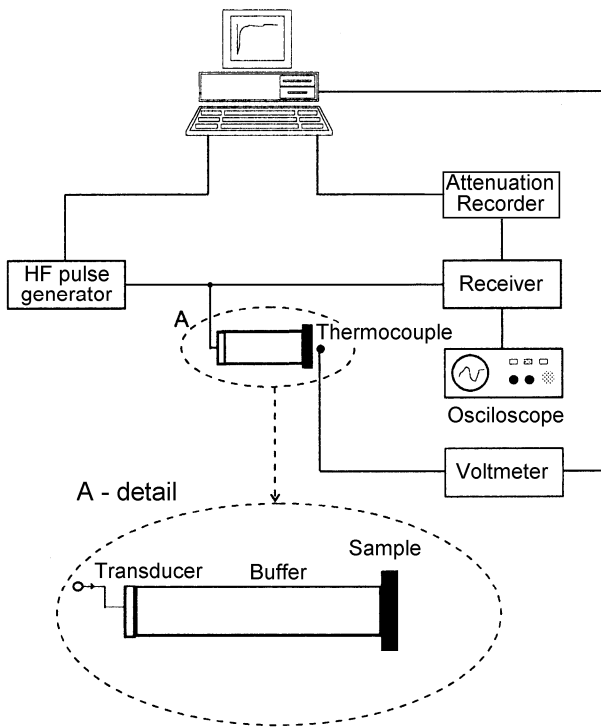

Fig. 1 Experimental arrangement for acoustic attenuation measurement

3.2. Acoustic transient spectroscopy of semiconductor interfaces

The present measurement technique of A-DLTS is based on the computer-evaluated transients measured at fixed temperatures [10]. The differential ARS or TAS, δU_{ac} can be then monitored as a function of temperature and peaks with maxima for which the emission rate is the same as the adjusted sample rate are observed in A-DLTS spectra. Using the well know relation expressing the temperature dependence of the relaxation time characterizing the AE transient [9], the activation energy, E_T, and corresponding capture cross-section, σ, can be determined.

A block diagram of the experimental arrangement of the A-DLTS technique is shown in Fig. 2. The computer system was used to trigger the apparatus – Pulse Modulator and Receiver, to generate excitation bias pulses as well as to record and evaluate the isothermal transient of the ARS. A SAW of frequency 10 MHz was generated using an interdigital transducer evaporated on the LiNbO$_3$ delay line and the structure to be investigated was placed on the top of the LiNbO$_3$ and pressed against the selected window (detail-A). A longitudinal acoustic wave of frequency 13.2 MHz was generated using a LiNbO$_3$ transducer in the arrangement illustrated in the B-detail. The ARS produced by the MOS (Metal-Oxide-Semiconductor) structure after detection in the SRS Gated Integrator and Box-car Averager was then recorded and stored by computer.
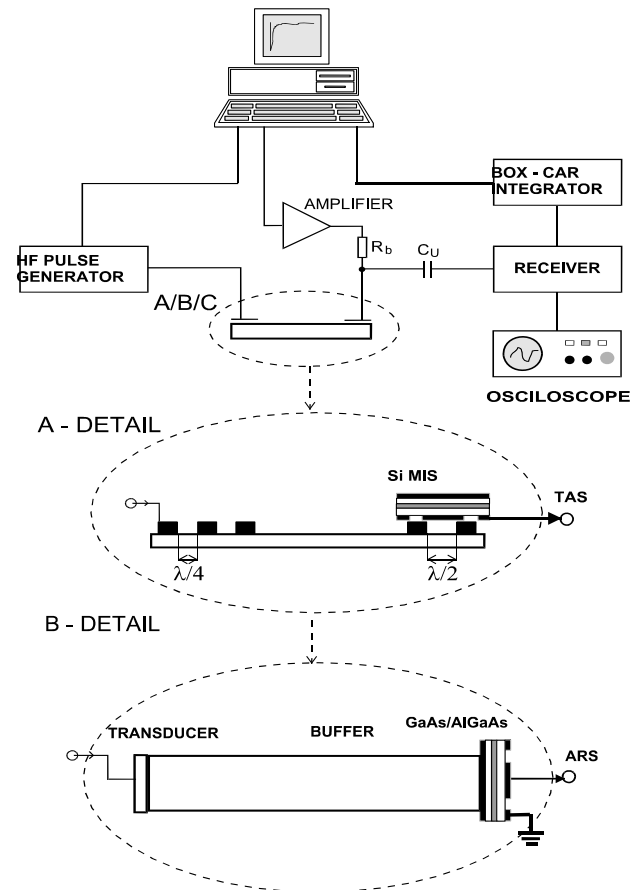

Fig. 2 Block diagram of the experimental arrangement for A-DLTS measurements. The detailed sample configurations are illustrated in A-detail (TAS measurement) and B-detail (ARS measurement).

3.3. Acoustic spectroscopy of magnetic fluids

The block diagram of the experimental arrangement for magnetic fluids investigation is similar as is shown in Fig. 1, however the measured sample is magnetic fluid placed in measuring cell situated between the electromagnet poles. An acoustic pulse propagating in the measuring cell (1,5 x 1 x 1 cm^3) underwent a multiple reflection from the transducers and its subsequent echoes were recorded. Measurements of the changes of the absorption coefficient of acoustic wave were carried out by a pulse method. Two selected adjacent pulses following separate paths reach a detector from where signals proportional to their amplitudes are fed to a attenuation recorder. The signal from attenuation recorder, which is proportional to the changes of the acoustic wave absorption coefficient in a given medium was measured by a digital multimeter.

4. RESULTS AND DISSCUSION

4.1. Acoustic transient spectroscopy of phosphate glasses

The representative acoustic spectra measured at 18 and 27 MHz of some glasses of the System I are illustrated in Fig. 3.
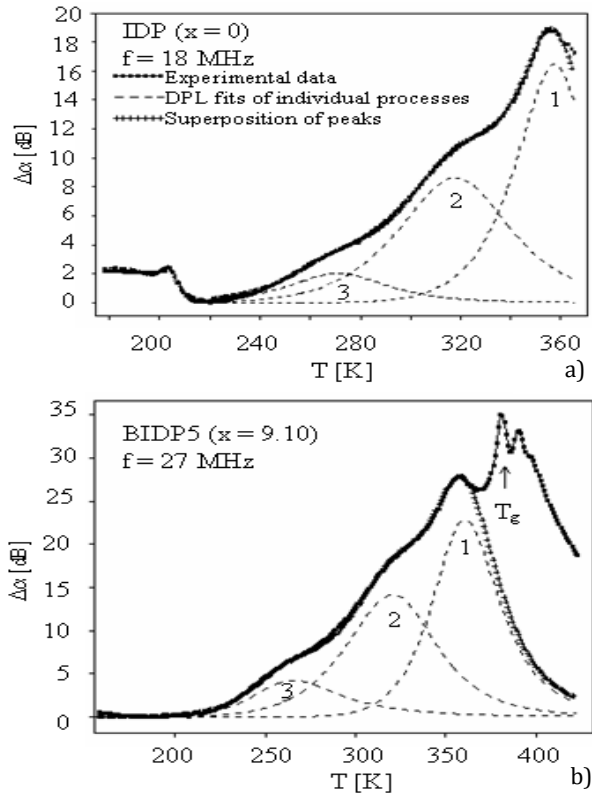
Fig. 3 Representative acoustics attenuation spectra of two glasses of the System I, measured at 18 MHz and 27 MHz. Cross-marked lines represent the best fit as superposition of individual peaks (dashed lines).

The acoustic attenuation spectra of all samples from investigated set at all frequencies indicate one broad attenuation peak at higher temperature in which we can distinguish easily two separated peaks. Using the Arrhenius type equation between the peak temperature T_{peak} and the applied frequency f (1) the value of activation energy of the ion hopping process can be determined.

The acoustic attenuation spectra of the investigated cuprous halide glasses were gradually fitted using various theoretical attenuation functions including the Debye, Kohlrausch-Williams-Watts and Double Power Law functions utilizing the mathematical procedure of genetic algorithm with binary representation of the theoretical attenuation function variables [15]. Using the theoretical model with Double Power Law function (5), calculated lines gave an excellent agreement with the measured acoustic spectrum in the whole temperature range.

The acoustic attenuation spectra were finally analyzed assuming the existence of three thermally activated relaxation processes of Cu^+ ions in connection with different kinds of sites [14]. The proportion of the intensities of first two peaks (I_1 / I_2) depends on the glass composition, that is on the ratio CuBr/(CuI + CuBr) and reaches its maximum at x = 6.82 similarly as dc conductivity. The third peak, the presence of which only enables to fit the experimental dates thoroughly, represents non-essential transport mechanisms probably dependent only on glass forming system. Using the equation (1) and values of T_{peak} for individual peaks, the activation energies E_a^a were determined. In addition to

relaxation studies, for each glass of System I the glass transition temperature, T_g, was observed from acoustic attenuation measurement. The activation energies corresponding to individual peaks have the values E_{a1} = 0.46 – 0.48 eV, E_{a2} = 0.41 - 0.43 eV and E_{a3} = 0.36 – 0.39 eV, respectively. Quite good correlation was found with the results obtained by conductivity measurements, however some new features were observed, too.

The results from IR spectra of the CuI-$CuBr$-Cu_2O-P_2O_5 glasses [15] indicate that the thermal activated processes of Cu^+ ions determined for all samples of investigated systems can be associated mainly with three different structural units - monomeric orthophosphate PO_4^{3-}, low-condensed dimeric diphosphate oxoanions $P_2O_7^{4-}$ and $P_3O_{10}^{5-}$ structure phosphate anions.

The infrared study of Cu^+ ions conducting glasses in the similar systems as System II showed that these glasses contain mainly PO_4^{3-} and MoO_4^{2-} tetrahedral anions groups and cuprous halides as well as their mixtures do not affect significantly the dominant phosphate and molybdate oxide structural units of glasses.

4.2. Acoustic transient spectroscopy of Si MOS strucstures

Using the above-described techniques the development of both the ARS and hf TAS as a function of temperature after the proper injection pulse was investigated in Si MOS structures and their A-DLTS spectra were constructed.

Ultrathin silicon dioxide (SiO_2) layers formed on Si substrate with nitric acid have been investigated using acoustic deep-level transient spectroscopy (A-DLTS) to characterize the interface states. The set of SiO_2/Si structures formed in different conditions (reaction time, concentrations of nitric acid (HNO_3), and SiO_2 thickness [3-9nm] was prepared [see Tab. 1]. The leakage current density was decreased by post-oxidation annealing (POA) treatment at 250°C in pure nitrogen for 1 h and/or post-metalization annealing (PMA) treatment at 250°C in a hydrogen atmosphere for 1 h [16].

Table 1 Summary of the investigated (hAl/SiO2/ Sii) MOS structures [17]

Sample No.	1	2	3	4	5	6	7
Thickness[*] (nm)	2.7	3.2	9.2	3.2[**]	3.8	2.9[**]	3.5[**]
Reaction time (h)	7.5	6	10	4	10	3.5	4
Concentration of HNO_3 [%]	53	58	58	58	68	62	62

[*] estimated from XPS or [**] elipsometry measurements

Fig. 4 shows the representative A-DLTS spectra of two MOS structures, (a) sample No. 5 and (b) sample No. 6, exposed to both POA and PMA treatments. The illustrated spectra that contain only one peak, corresponding to one interface state, were measured at reverse bias V_G = -0.5 V with pulse voltage ΔV_G =1.2 V and the same time constant. The activation energies and the corresponding capture cross-sections were determined

from the Arrhenius plots constructed for individual peaks. It is evident that A-DLTS peaks represented by MOS structures with PMA, are much lower then those with POA treatment. Summary of all observed interface states, their activation energies, and corresponding cross-sections is in Tab. 2.
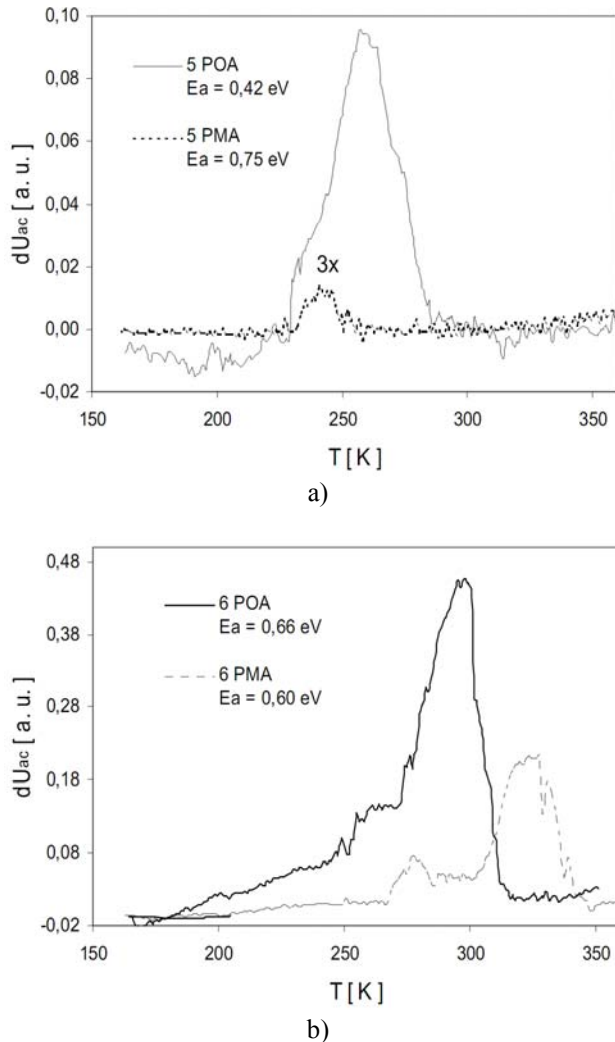

a)

b)

Fig. 4 A-DLTS spectra of two SiO_2/Si structures: a) No. 5 (3.8 nm SiO_2); b) No. 6 (2.9 nm SiO_2) for the same relaxation time (τ = 43.6 ms) at V_G = 0.5 V and V_G = 1.2 V, treated by both POA and PMA

Table 2 Summary of interface states determined from A-DLTS spectra and leakage current density at -2 V

Sample	Ea [eV]	$\sigma[cm^2]$	LCD* at -2V [Acm^{-2}]
1POA	0.4	1.27×10^{-17}	3×10^{-4}
1PMA	0.31	8.26×10^{-18}	8×10^{-7}
2POA	0.66	9.78×10^{-14}	9×10^{-5}
2PMA	0.81	9.24×10^{-11}	2×10^{-7}
3POA	0.64	1.40×10^{-14}	3×10^{-3}
3PMA	not	detected	1×10^{-3}
4POA	0.42	4.58×10^{-17}	5×10^{-3}
4PMA	not	detected	1×10^{-6}
5POA	0.42	4.52×10^{-16}	1×10^{-5}
5PMA	0.75	4.8×10^{-9}	8×10^{-6}
6POA	0.6	1.10×10^{-15}	2×10^{-3}
6PMA	0.66	1.23×10^{-13}	2×10^{-5}
7POA	0.16	4.0×10^{-20}	1×10^{-4}
7PMA	not	detected	6×10^{-6}

- LCD = Leakage current density

The A-DLTS spectra of PMA structures definitely indicate the lower concentration of interface states compared with POA structures, represented by smaller or even an undetected A-DLTS peak. Except for a lower concentration of interface states in the structures with PMA compared with POA structures, the shift of their activation energies above or below the midgap was observed. This indicates that the some interaction of Si dangling bonds with hydrogen, Si, or oxygen atoms in the SiO_2 layer can occur during the PMA treatment, as well as the reaction between the Al atoms and SiO_2, producing the Al_2O_3 layer.
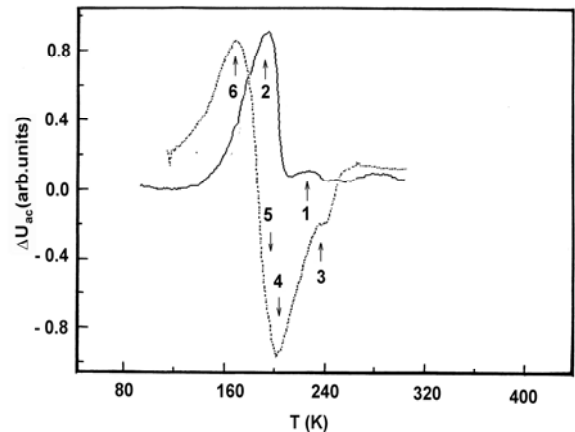

Fig. 5 A-DLTS spectra, obtained by SAW technique, of Si(n) (full line) and Si (p) (dotted line) MOS structures

Fig. 5 shows typical A-DLTS spectra obtained for Si MOS structures prepared by CVD technique on both n- and p-type Si substates to thickness 80 nm obtained by A-DLTS technique using the hf TAS. Using the above mentioned procedure, the activation energies and capture cross-sections, were calculated (Tab. 3). The obtained values are mostly in good agreement with the values found by DLTS or others techniques [8.17].

Table 3 Summary of the deep centers parameters detected by SAW A-DLTS in Si MOS structures

Label	Structure	E[eV]	$\sigma[cm^2]$	-U_G[V]
1.	Si(n) MIS	0.37	7.8×10^{-17}	3.0
2.	Si(n) MIS	0.21	4.7×10^{-19}	3.0
3.	Si(n) MIS	0.49	3.3×10^{-13}	4.0
4.	Si(p) MIS	0.67	5.2×10^{-11}	4.0
5.	Si(p) MIS	0.47	6.5×10^{-13}	4.0
6.	Si(p) MIS	0.61	3.4×10^{-6}	4.0

4.3. Acoustic properties of magnetic fluids

The investigated magnetic fluid used in experiments consisted of magnetite particles ($FeO.FeO_2O_3$), the mean diameter D = 10.69 nm, coated with oleic acid as a surfactant, dispersed in inhibited transformer oil ITO 100. The basic properties of this magnetic fluid, such as the density, saturation magnetization and volume fraction are equal to 1.071 g/cm^3, 8.81 mT and 2 %, respectively. The acoustic velocity of magnetic fluid without magnetic field is c = 1652 m/s (25 °C).

The measurements were recorded at the acoustic wave of frequencies 5 and 17 MHz, for the direction of acoustic wave propagation parallel to the direction of the external magnetic field. The magnetic field in the range 0 – 450 mT was changed in steps 10 mT every 30 second (the whole sweep time - 25 min).

Fig. 6 presents the changes of the acoustic wave absorption coefficient $\Delta\alpha$ for the both acoustic wave of frequency 17 MHz and 5 MHz as a function of the magnetic field and for **B || k**.
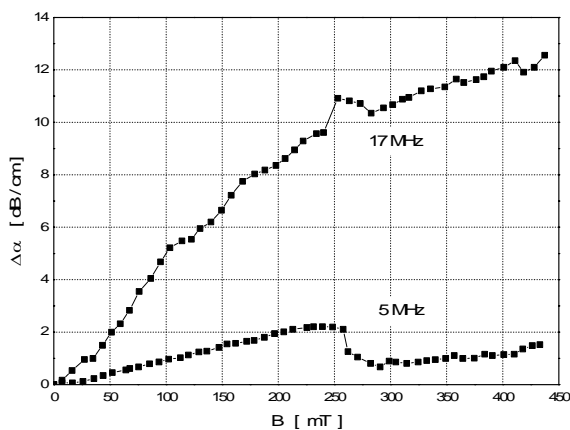

Fig. 6 Experimental data of changes in the acoustic wave attenuation as a function of the increasing magnetic field for two frequencies

These results show a strong influence of the steeped magnetic field on the value of acoustic attenuation. With increasing magnetic field, the acoustic wave absorption increases. When the magnetic field is swept at a constant rate, the dominant interactions occur between the external magnetic field and the magnetic moment of the particle, leading to aggregation of particles and the clusters are formed. These effects caused the increase of the absorption of acoustic wave with increasing magnetic field.

At magnetic field around 260 mT it was observed a maximum of $\Delta\alpha$ at 5MHz and a peak at 17 MHz, which appear as a result of the additional resonance absorption of the acoustic wave by the spherical clusters.

The character of absorption coefficient changes is different with decreasing magnetic field when the changes of the acoustic wave absorption coefficient show a hysteresis. This effect can be described by existence of clusters, which lifetime was longer than time of decrease of the magnetic fluid. The structure does not return to the initial state immediately after the magnetic field has been removed.

5. CONCLUSIONS

In conclusion, the presented methods of acoustic spectroscopy applied to several kinds of materials and/or structures evidently documented that the method can be a powerful facility to obtain important informations about investigated material properties. Both the solid glassy electrolytes and MOS interfaces investigation offer the informations about their physical properties which can complete the data obtained using different, mostly electrical methods. The acoustic spectroscopy of magnetic fluids provides also additional data about magnetic and structural properties under the various external conditions. The further development of techniques of acoustic spectroscopy and their application to various materials can bring new interesting informations about their properties and eventual applications.

ACKNOWLEDGMENTS

REFERENCES

[1] Physical Acoustics, Ed. By W. P. Mason and R. N. Thurston.: ACADEMIC PRESS, Vol. I, II. Seria 1964.

[2] Ultrasonic Instruments and Device, Ed. By P. Papadakis, ACADEMIC PRESS, 1999.

[3] INGRAM, M. D.: Glastech. Ber. Glass. Sci. Technol. 67, 151-155 (1994).

[4] ZNÁŠIK, P. – JAMNICKÝ, M.: Solis State Ionics 95, 207-214 (1989).

[5] ALMOND, D. P. – WEST, A. R.: Solid State Ionics 26, 265-278 (1988).

[6] CARINI, G. – CUTRONI, M. – FEDERICO, M. – GALLI, G. – TRIPODO, G.: Phys. Rev. B30, 7219-7224(1984).

[7] ABBATE, A. – MAN, K. J. – OSTROVSKIJ, I. V. – P. DAS: Solid State Electronics 36 (1993) 697.

[8] BURY, P. – JAMNICKÝ, I. – RAMPTON, V. W.: Physica B 263-264 (1999) 94.

[9] BURY, P. – JAMNICKÝ, I. – ĎURČEK, J.: Phys. Stat. Sol. (a) 126 (1991) 151.

[10] BURY, P. – JAMNICKÝ, I.: Acta Phys. Slovaca 46 (1996) 693.

[11] KÚDELČÍK, J. – BURY, P. – TIMKO, M. – BRAMANTYA, M. A. – MOTOZAWA, M. – TAKUMA, H. – FAIZM, M. – SAWADA, T.: Journal of Physics: Conf. Series 149 (2009) 012040.

[12] JÓZEFCZAK, A.: J. Magn. Magn. Mater. 294 (2009), in press.

[13] JAMNICKÝ, M. – ZNÁŠIK, P. – TUNEGA, D. – INGRAM, M. D.: J. Non-Cryst. Solids 185, 151-158 (1995).

[14] BURY, P. – HOCKICKO, P. – JUREČKA, S. – JAMNICKÝ, M.: Physica Status Solidi (c) 11 2888-2891 (2004).

[15] BURY, P. – HOCKICKO, P. – JAMNICKÝ, M.: Adv. Mater. Research 39, 111-116 (2008).

[16] BURY, P. – KOBAYASHI, H. – TAKAHASHI, M. – IMAMURA, K. – SIDOR, P. – ČERNOBILA, F.: Cent. Eur. J. Phys. 7(2), 2009, 237-241.

[17] AS, D. J. – EPERLEIN, P. W. – MOONEY, P. M.: J. Appl. Phys. 64, 2408 (1988).

[18] KÚDELČÍK, J. – BURY, P. – ZÁVIŠOVÁ, V. – TIMKO, M. – KOPČANSKÝ, P.: Proc. Scientific Conf. Physics of Materials, Košice 2009. pp. 91-93.

BIOGRAPHIES

Peter Bury received the M.Sc. in experimental physics in 1972 and PhD. in 1982 at the Faculty of Natural Sciences (Faculty of Mathematics and Physics), Comenius University, Bratislava. Currently he is Professor of Physics of Condensed Matter and Acoustics at Department of Physics, Faculty of Electrical Engineering, Žilina University. The most of his research work was orientated on the study of semiconductors and semiconductor structures using acoustic methods. Formerly he investigated Cr states in GaAs using APR technique, later deep centers in both semiconductor and semiconductor structures using acoustic transient spectroscopy (A-DLTS). Currently h of $\Delta\alpha$ e used methods of acoustic spectroscopy also to study glasses, ferroelectrics and magnetic fluids.